Acoustic Properties of Fluid-Saturated Blood Clots

by Pierre D. Mourad and Steven G. Kargl

Technical Report
APL-UW TR 2003
September 2000

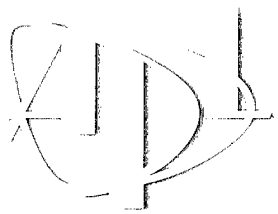

Applied Physics Laboratory University of Washington
Seattle, Washington 98105-6698

ONR Contract N00014-96-1-0630

ACKNOWLEDGMENTS

Our work has benefited from discussions with Dr. Charles Francis of the University of Rochester, Dr. E. Carr Everbach of Swarthmore College, and the Physical Acoustic Group at the Applied Physics Laboratory, University of Washington. Funding for this work was provided by the Defense Advanced Research Projects Agency under the management of the Office of Naval Research.

ABSTRACT

Ultrasound has been applied to blood clots to enhance enzyme-mediated thrombolysis through unknown mechanisms. A basic physical description of a blood clot is a two-phase medium composed of a saturating fluid and an interconnected network of elastic material. Acoustic wave propagation in a fluid-saturated, poroelastic medium can be represented by Biot's theory. The question therefore arises, Might blood clots support the propagation of sound in a way consistent with Biot's theory? We address this question by first surveying the literature for measurements of the physical properties of blood clots that are needed to apply Biot's theory. We discuss the strengths and weaknesses of these measurements, and determine a useful set of values for modeling. Using these parameter values, we then calculate the phase velocities and absorption coefficients of the three waves predicted by Biot's theory for various types of blood clots in an unbounded medium.

CONTENTS

LIST OF FIGURES

LIST OF TABLES

1. INTRODUCTION

In vitro and *in vivo* experiments have shown that ultrasound accelerates enzyme-mediated thrombolysis [1–11]. One mechanism for this enhanced thrombolysis is the microstreaming that accompanies bubbles resulting from cavitation. However, cavitation *in vivo* is unlikely because of the high pressure threshold for cavitation in whole blood relative to the acoustic conditions typically used for ultrasound-assisted thrombolysis [12]. Moreover, recent *in vitro* studies show ultrasonic acceleration of enzyme-mediated thrombolysis even when cavitation is suppressed by degassing the saturating fluid and applying an overpressure [13,14]. Everbach et al. [13] and Blinc et al. [5] show that a thermal mechanism cannot account for the thrombolysis observed *in vitro* after cavitation is suppressed. Blood clots can be described as fluid-saturated poroelastic media [15]. Hence, we hypothesize a nonthermal and noncavitational mechanism based on Biot's theory. The salient characteristic of this proposed mechanism is that ultrasound causes the saturating fluid to move relative to the underlying network of fibrin fibers, which permits advection as well as diffusion of clot-lysing agents.

Biot [16, 17] developed a theory for the propagation of linear acoustic waves in a fluid-saturated poroelastic medium. He was originally concerned with wave propagation in soil, which he treated as an elastic skeletal frame and a saturating fluid on an equal footing. That is, the dynamic behavior of the fluid and the skeletal frame were included independently by considering the displacements and stress tensors of the underlying constituents. Since the pioneering work of Biot, others have applied this theory to many diverse fluid-saturated poroelastic structures such as rocks and synthetic sandstones [18], sea sediments [19], and gels [20]. A general review of the theory has been given by Johnson [21].

A homogeneous fluid supports a single compressional wave while a homogeneous, isotropic elastic medium supports a compressional wave as well as coupled and uncoupled shear waves. A remarkable feature of Biot's theory is the presence of two, distinct compressional waves as well as coupled and uncoupled shear waves. The dynamics of the shear waves predicted by Biot's theory are similar to those predicted by elasticity theory (with an appropriate definition of the phase velocity for the shear waves). The compressional waves are commonly referred to as the fast wave and the slow wave because of their respective phase velocities. Typically, the phase velocity of the fast wave lies between the compressional phase velocities of the elastic constituent and the fluid constituent. The phase velocity of the slow wave is generally less than the compressional phase velocity of both constituents.

As the fast wave propagates through a fluid-saturated poroelastic medium, the fluid and the skeletal frame compress and expand nearly in-phase and in the direction of propagation. That is, the fluid and skeletal frame move in the same direction at the same time with a slight phase offset. For the slow wave, the fluid and the skeletal frame move largely out-of-phase, nearly in opposite directions. For the shear waves (i.e., waves in the plane transverse to the direction of propagation), the fluid and the skeletal frame exhibit nearly in-phase relative motion. *A key feature of all of the waves manifest by Biot's theory is that the saturating fluid moves relative to the skeletal frame.* This suggests that the enhancement of enzyme-mediated thrombolysis by the application of ultrasound may be due to enhanced transport, by advection, of clot-lysing agents within the blood clot. The purpose of this report is to lay the theoretical foundation necessary to build a predictive model of this hypothesis.

In Section 2, we summarize an extensive literature search for the material properties of saturated blood clots, the saturating fluid (plasma and serum), and the fibrin fibers. In Section 3, a representative set of parameters for a whole-blood clot is used with Biot's theory to predict the phase velocities and absorption coefficients for fast, slow, and shear waves. Conclusions are given in Section 4. A concise mathematical formulation of Biot's theory has been given by Kargl et al. [22] and will not be repeated here.

2. DETERMINING MATERIAL PARAMETERS

Determining the acoustic properties of a fluid-saturated poroelastic medium via Biot's theory requires a minimum of ten physical parameters [21–23]. The first three parameters describe intrinsic properties of a poroelastic medium. These parameters are the porosity, hydrostatic permeability, and tortuosity, which are designated as β, K_d, and α, respectively. The next three parameters pertain to the saturating fluid. These parameters are the density, dynamic viscosity, and bulk modulus, which are denoted by ρ_f, η, and K_f, respectively. For the blood clots considered here, the fluid is serum (i.e., fibrinogen-free plasma). The final four parameters describe the viscoelastic properties of the elastic constituent and the drained skeletal frame. A "drained skeletal frame" is the elastic medium after removal of the saturating fluid but retaining the porous structure. The elastic constituent is fibrin, and its density and bulk modulus are denoted by ρ_e and K_e. The viscoelastic behavior of the drained skeletal frame is parameterized by a bulk modulus, K_b, and a shear rigidity, N.

We were able to gather together representative values of these parameters from the literature for four types of clots: whole-blood clots, plasma blood clots, coarse fibrin gels, and fine fibrin gels. Whole blood clots occur both *in vivo* and *in vitro*, whereas the other types of clots are used only for *in vitro* studies. A whole-blood clot has within it not only fibrin and serum, but also platelets and occasional red and white blood cells. The net effect is that whole-blood clots are the stiffest and most permeable of the four types. A clot made from plasma is free of erythrocytes and platelets. Coarse fibrin gels are composed of serum and fibrin. They have a permeability that can rival that of whole blood clots, although they have a weaker frame. Fine fibrin gels are the least permeable and least resistant to stress. The gels are often used as *in vitro* models of blood clots because fibrin gels are easy to handle and have the most easily reproducible structure. We compiled the required parameters from a variety of references because we could not find an individual reference that gave all of these quantities for a single clot or clot type. This is not surprising because previous researchers have not investigated a paradigm based on Biot's theory as a mechanism for ultrasound-assisted thrombolysis.

2.1 Porosity, β

The porosity, β, of a porous medium is a measure of the relative percentage, by volume, of the pore space to the total volume of the sample. Values of β range from 0 to 1, with 1 being more vacuous and 0 being less vacuous. The porosity of a random packing of sand is nominally 0.38, whereas for almost all types of blood

clots the porosity is greater than 0.9. Rosser et al. [24] report that the porosity of coarse and fine fibrin gels is greater than 0.97. In a summary of observations of the porosity of a range of clot types, Anand et al. [25] report that β ranges from 0.75 to 0.99. This is a critical parameter for the application of Biot's theory to blood clots. For whole-blood clots, we use $\beta = 0.90$, for plasma blood clots $\beta = 0.97$, and for fine and coarse fibrin gels $\beta = 0.99$.

2.2 Hydrostatic Permeability, K_d

The hydrostatic permeability, or Darcy's constant, K_d, is a measure of how well a liquid flows through a permeable medium. The larger the value, the more permeable the medium. Hydrostatic permeability appears to vary by several orders of magnitude between types of clots and be highly variable even within a given type. Anand et al. [25] found $1 \times 10^{-12} \leq K_d \leq 1 \times 10^{-16}$ m^2 for a variety of clot types. Okada and Blomback [26] studied a variety of factors that affect fibrin gel structure. By measuring the flow of latex spheres through clots, they obtained good estimates for the pore sizes within the clots as well as the variance in those pore sizes. (The pore sizes ranged from hundreds of nanometers to a few microns, with a variance of about plus or minus five percent.) From the pore sizes, Okada and Blomback inferred $K_d \approx 1 \times 10^{-13}$ m^2 for a plasma clot, which is consistent with values reported by Anand et al. Carr and Hardin [27] show that when erythrocytes are present, the average pore size of fibrin gels is significantly increased, rivalling that of whole blood clots. Therefore, not only the ionic strength of the fibrinogen-thrombin solution (which also controls fibrin-mesh thickness) but also the presence or absence of cells such as red or white blood cells or platelets helps determine pore size, and hence hydrostatic permeability. Carr and Hardin give $K_d \approx 1 \times 10^{-12}$ m^2 as representative for clots made of whole blood, plasma, and fibrin when erythrocytes are present. The hydrostatic permeability of coarse and fine fibrin gels has been measured by Rosser et al. [24], who found $1 \times 10^{-13} \leq K_d \leq 1 \times 10^{-14}$ m^2 for coarse gels and $1 \times 10^{-15} \leq K_d \leq 1 \times 10^{-16}$ m^2 for fine gels. Carr et al. [28] provide independent estimates for these types of clots. Their values are $K_d \approx 5 \times 10^{-13}$ and 6×10^{-15} m^2 for coarse and fine fibrin clots, respectively.

For whole-blood clots, we use the value of $K_d = 1 \times 10^{-12}$ m^2 measured directly by Carr and Hardin for a well-characterized clot. The only direct measurement we could find of the hydrostatic permeability of clots made from plasma was $K_d = 1 \times 10^{-13}$ m^2 by Okada and Blomback, a plausible value. Finally, we use the values of $K_d = 5 \times 10^{-13}$ m^2 and $K_d = 6 \times 10^{-15}$ m^2 measured by Carr et al. for coarse and fine fibrin clots, which are consistent with the other measurements reported above.

2.3 Tortuosity, α

The tortuosity, α, of a porous material gives a measure of the structure and convolution of the pores within the material. It is an intrinsic geometric quantity that is greater than or equal to unity. When the pores within a porous material are uniform, straight, cylindrical tubes, then the tortuosity attains its lower limit of 1. As the pore geometry deviates from straight tubes, the tortuosity increases. Kargl and Lim [23] summarize various analytic and empirical results that relate the tortuosity to porosity for a given microstructure of a porous material. Micrographs of various types of clots indicate that the fibrin mesh is composed of a random formation of thin, cylindrical bundles of fibrin [15]. This suggests that the analytic result for a self-similar random array of needles may provide an adequate estimate for the tortuosity of blood clots, which Table I of Kargl and Lim puts between 1.01 and 1.1.

2.4 Density of Plasma and Serum, ρ_f

Duck [29] gives a solid measure of the density of plasma, $\rho_f = 1027\ \mathrm{kg/m^3}$, which we use for our calculations. This value is adequate for serum because the protein content of plasma will make a negligible contribution to the density compared to the uncertainty in the other measured quantities.

2.5 Dynamic Viscosity of Plasma and Serum, η

There are a number of references that give the dynamic viscosity, η, of plasma and serum, including articles by Watson [30] and Shearn et al. [31,32], who considered the effects of disease, and Duck [29], who gives a fairly exhaustive survey of the literature. All of these references are for shear rates that are, with one exception, much too small to be relevant to our study. In addition, most researchers work with biological fluids at temperatures that are well below a body temperature of 37°C.

Rosenson et al. [33] measured the dynamic viscosity of whole blood, plasma, and serum in healthy adults in order to establish a baseline against which to compare the corresponding dynamic viscosity of blood and blood products of people with diseases. The shear rates that they considered are those that are generally manifest within blood vessels and are considerably lower than those induced by ultrasound. However, they did keep their experimental fluids at body temperature. They observed no non-Newtonian behavior in plasma or serum, but did so in blood. Their values of 1.27 ± 0.06 millipoiseuille (mPl) for serum and 1.38 ± 0.08 mPl for plasma appear to

be a good upper bound for the dynamic viscosity.

Merrill and Wells [34] present a detailed and excellent discussion of the generally non-Newtonian behavior of a variety of biological fluids, with a strong emphasis on blood and blood products. They discuss the biological basis for those results, generally in terms of the multiscale relaxation of macromolecules (and cells where appropriate) within the fluids. Merrill and Wells report $\eta = 1.17$ mPl for plasma, but their data were restricted to shear rates that are too low for our purposes. However, they reference other work with shear rates up to 20 kHz for plasma in which the measured dynamic viscosity was 1.04 mPl and appeared to be constant above 3 kHz. We have chosen 1.04 mPl for the value of dynamic viscosity of serum because the measured value for plasma was constant over a wide range of relatively high shear rates, the dynamic viscosity of plasma and serum are comparable at low shear rates, and there is a lack of other more relevant data.

2.6 Bulk Modulus of Plasma and Serum, K_f

We could not find measured values of the bulk modulus, K_f, and the sound speed, c_f, of serum. However, we were able to find the speed of sound in plasma, from which we can determine its bulk modulus. Because serum is plasma without fibrinogen, we chose the sound speed value for the plasma that contained the least amount of proteins to approximate the sound speed of serum and hence its bulk modulus. Carstensen and Schwan [35] measured both absorption and sound speed in a variety of hemoglobin solutions created from blood from different mammals. They systematically varied the percentage of hemoglobin in the solutions and developed a mathematical model of the absorption based on the concept of multiscale relaxation processes. Carstensen and Schwan report $c_f = 1608$ m/s for a solution containing free beef hemoglobin at whole-blood protein levels. Unfortunately for the present work, the temperature of their experimental hemoglobin solutions was 25°C. However, they did see a reduction in sound speed with a reduction in the amount of free hemoglobin, which is a trend that also shows up in plasma. Their results are interesting because they show that increasing the level of protein increases the sound speed of blood products. Collings and Bajenov [36] measured the sound speed in human blood and plasma over a large range of frequencies (all higher than necessary for our current study) and over a large range of temperatures that included body temperature. They report a sound speed of 1550 m/s at a frequency of 2.67 GHz for a plasma containing 0.0516 g/ml of protein at 37°C. Their results seem to be a good upper bound for the sound speed of serum because of the general trend for sound speed to increase with both protein content and frequency and their observation that the sound speed in plasma was independent of frequency in the range that they considered. Aubert et

al. [37], referenced by Duck [29], give perhaps the best estimate for the sound speed in serum, $c_f = 1530$ m/s, because their plasma contained a relatively small amount of protein (0.0129 g/ml) and the frequency range (1–10 MHz) and temperature (37°C) were appropriate. This value of sound speed is consistent with the effects of frequency and protein content reported in other references.

The bulk modulus is obtained from $K_f = \rho_f c_f^2$, where $c_f = 1530$ m/s and density $\rho_f = 1027$ kg/m^3, as given in Section 2.4. This yields $K_f \approx 2400$ MPa. As a comparison, the bulk modulus of fresh water is approximately 2250 MPa at room temperature and one atmosphere ambient pressure.

2.7 Density of Hydrated Fibrin, ρ_e

There is a paucity of references for the density of hydrated fibrin, ρ_e (indeed, for protein in general). Ferry and Morrison [38] report the only direct measure of fibrin density that we could find, in an elegant and intuitive analysis. In order to determine the density of fibrin, they constructed fibrin films with an ever-increasing ratio of fibrin to saturating liquid for a variety of liquids (water and water/glycerol mixtures). They then allowed the fibrin films to float in the different liquids. By calculating the amount of displaced fluid in each case, they inferred the density of the films. As the ratio of fibrin to liquid increased, the inferred density increased to 1300 kg/m^3 for films made out of 100% fibrin. There is, however, some uncertainty in that value because the pressure applied to the fibrin to produce the films was not enough, by their analysis, to drive the liquid entirely out of the fibrin fibers. This suggests that there was still liquid saturating the fibrin fibers at what they report to be a concentration of 100% fibrin. Thus, their value of approximately 1300 kg/m^3 for the density of 100% fibrin is probably more appropriate for the density of saturated fibrin.

Carr and Hermans [28], Voter et al. [39], and Carr (personal communication, 1998) give a value of density that is a measure of the actual protein concentration within a fibrin fiber, rather than a measure of how well or poorly a fibrin fiber will float. Carr and Hermans report that proteins take up about 20% of the volume of fibrin, with serum taking up the rest. Their research indicates that fibrin is denser than serum, without quantifying the value of that density. Voter et al. find a comparable value for protein concentration, with the percentages of fibrin and serum depending on the ionic strength of the fluid during clot formation. As discussed in Section 2.8, Kaibara et al. [40] show that the structure of the fibrin in a clot (e.g., the porosity and the thickness of fibrin strands) varies significantly, depending on the ionic strength. Therefore, it is likely that the density of fibrin varies with clot type. We used Ferry

and Morrison's value of $\rho_e = 1300$ km/m^3 [38]. However, because the density of fibrin is a crucial parameter in Biot's theory, and because the measurements of Ferry and Morrison [38] were made before a thorough appreciation of how the structure of clots varies with ionic strength, better and wider-ranging measurements of fibrin density are required to refine the predictions from Biot's theory.

2.8 Shear Rigidity of Saturated Clots

The shear rigidity of a material is a measure of how well that material resists shear forces. The larger the shear rigidity, the more resistant that material is to deformation due to shear forces. The shear rigidity is a well-studied quantity for a range of clot types. Motivation for that work includes the desire to explore variations in the strength of cross-linking between fibrin fibers under a variety of physiologically relevant conditions and to see how various drugs and chemicals affect the ability of a clot to resist shear stress. Unfortunately, these studies all consider very small shear rates relative to our current needs, and many of these studies were performed at room temperature. However, the values reported for shear rigidity are sufficiently small that large uncertainties in these value would not alter our calculations. Kaibara and Fukada [41] show that the shear rigidity decreases with increasing temperature for clots made from whole blood and plasma that are subjected to a periodic strain (about 10 Hz) throughout their formation. They also show that the decrease is on the order of 10 to 20%. While not directly relevant, these values can be taken as an upper bound, at least for these low shear rates.

Measurements of the shear rigidity of clots made from whole blood are reported in various references. Overholser et al. [42] report a value of $300 - \imath 10$ Pa, where the complex-valued shear rigidity is a manifestation of an intrinsic absorption loss. This measurement was performed with whole blood at body temperature. Kaibara and Fukada [43] found a range of values from $100 - \imath 10$ Pa to $150 - \imath 30$ Pa, but their measurements were conducted at room temperature. Kamykowski et al. [44] measured the shear rigidity of a variety of clot types; however, they provide only the real part of the shear rigidity, which ranges from 70 to 2600 Pa, and their measurements were conducted at room temperature. Hence we use the value of $300 - \imath 10$ Pa given by Overholser et al. for whole-blood clots to constrain the inversion procedure described in Section 2.9.

Kaibara and Fukada [41, 45] report two measurements of the shear rigidity of a clot formed from a plasma at room temperature. In their first paper, they report a shear rigidity greater than $22.5 - \imath 2.5$ Pa, while in the second paper they state a value of $800 - \imath 200$ Pa. Furthermore, they observe that for clots subjected to a periodic

strain throughout their formation, those made from whole blood have a larger shear rigidity than those made from plasma. They say that this is due to the presence of cells within the clot. However, the one value they report for the shear rigidity of a plasma clot not subjected to periodic strain throughout its formation is larger than that reported by others for whole blood under the same conditions. The lesson here is that the shear rigidity of clots is small but varies significantly, depending on the conditions during formation.

We could find only one paper that discussed the shear rigidity of coarse fibrin gels. The shear rate was the highest reported in any of the papers we could find on the shear rigidity of clots, and the shear rigidity was one of the highest of any clot type: $1000 - i100$ Pa.

Rosser et al. [24] also give values for the shear rigidity of fine fibrin gels at relatively high shear rates. These data provide perhaps the best estimate for the shear rigidity applicable to ultrasonic clot lysis. Their result of $400 - i80$ Pa is consistent with the results of Nelb et al. [46] measured under static rather than periodic strain. In addition, Nelb et al. report only a real-valued shear rigidity, which ranges from 100 to 1000 Pa. These measurements are the only indication we have that the shear rigidity is frequency independent. Unfortunately, two measurements are inadequate to determine the frequency dependence of shear rigidity.

Kaibara et al. [40] describe how the shear rigidity of a fibrin gel and the associated structure of the fibrin frame change with the ionic strength of the fibrinogen-thrombin solution. At low and high ionic strengths, the fibers that make up the frame of the clot are thick owing to the aggregation of fibrin bundles, creating a coarse fibrin gel whose shear rigidity is maximal. At intermediate ionic strengths, the clot frame is made up of thin fibers (protofibrils, or fibrin bundles), producing a fine fibrin gel with a shear rigidity about 20% smaller than that at low and high ionic strengths. The difference appears to be due to the relative number density of molecular bonds in the fibrin frame.

Finally, Kamykowski et al. [44], Kaibara et al. [40], Nelb et al. [46], and Bale et al. [47] all give values for the shear rigidity of a variety of clot types that are consistent with a shear rigidity ranging between 100 and 1000 Pa, again for a very small or zero shear rate. Unless the shear rate has a significant frequency dependence, the shear rigidity of a blood clot appears to be much smaller than its bulk modulus (another poorly determined quantity), and thus we can expect that blood clots do not support the propagation of shear waves at megahertz frequencies. This hypothesis is borne out by our calculations.

The measurements of shear rigidity just discussed involved clots containing a saturating fluid and low shear rates. At these shear rates, the dynamic viscosity would have a negligible effect on the measured shear rigidity. Therefore the majority of the shear stress should be supported by the fibrin frame. For clots made from whole blood, we use the value of $300 - i10$ Pa measured by Overholser et al. [42]. For clots made from plasma, we use $800 - i200$ Pa as measured by Kaibara and Fukada [41]. For both coarse and fine fibrin gels, we use $1000 - i100$ Pa as found by Rosser et al. [24]. The real parts of these values of shear rigidity are used to constrain an inversion procedure described in Section 2.9, and as such are not directly used within the framework of Biot's theory.

2.9 Bulk Moduli for Hydrated Fibrin and Drained Skeletal Frame, K_e and K_b

Direct measurements of the bulk moduli of an isolated hydrated fibrin fiber, K_e, or a drained skeletal frame, K_b, for any clot type are unavailable from the literature. To estimate K_e and K_b, we implemented an inversion procedure based on effective medium theories for elastic composites [48, 49]. Effective medium theories reduce the complexity of a composite material while capturing the macroscopic dynamics. A fluid model for a blood clot, for example, requires only the density and sound speed to describe compressional wave propagation, and knowledge of the complicated microstructure can be ignored.

Throughout the inversion, we assume that the density of the saturating fluid is $\rho_f = 1027$ kg/m^3 (Section 2.4), the density of an isolated fibrin fiber is $\rho_e = 1300$ kg/m^3 (Section 2.7), and the bulk modulus of the saturating fluid is $K_f = 2400$ MPa (Section 2.6). The inversion is constrained by the measured porosity given in Section 2.1 and the shear rigidities of various saturated clot types given in Section 2.8. In the following discussion, a "saturated clot" refers to a blood clot composed of a network of fibrin fibers and completely saturated by a fluid. A "drained clot" refers to a clot in which the saturating fluid has been removed while maintaining the structure of the fibrin fiber network (which we refer to as a "drained skeletal frame").

On a long enough length scale, a fluid-saturated blood clot can be treated as an effective medium. The Hashin-Shtrikman (HS) bounds [50–52] are rigorous lower and upper bounds on any estimate of effective elastic moduli for a composite medium composed of n constituents. The HS bounds are based on a variational analysis and depend on only the material parameters and volume fraction of each constituent. All other effective medium theories require additional information about the composite such as the orientation and shape of the microstructure. Let K_i and μ_i denote the

bulk modulus and shear rigidity for the ith constituent. Then, for a composite with only two elastic constituents, the lower HS bounds on the bulk modulus, K_l, and shear rigidity, μ_l, are determined from

$$\frac{1}{K_l + a_1} = \frac{c_1}{K_1 + a_1} + \frac{c_2}{K_2 + a_1} \tag{1}$$

and

$$\frac{1}{\mu_l + F_1} = \frac{c_1}{\mu_1 + F_1} + \frac{c_2}{\mu_2 + F_1}, \tag{2}$$

where c_1 and $c_2 = 1 - c_1$ are the volume concentrations of the individual constituents, $a_1 = 4\mu_1/3$, and $F_1 = [\mu_1(9K_1 + 8\mu_1)]/[6(K_1 + 2\mu_1)]$. Equations (1) and (2) are subject to the restrictions that $0 \leq K_1 \leq K_2$ and $0 \leq \mu_1 \leq \mu_2$. If constituent one is an inviscid fluid such that $\mu_1 \equiv 0$ and constituent two is an elastic material, then Eq. (1) reduces to

$$\frac{1}{K_l} = \frac{c_1}{K_2} + \frac{c_2}{K_2} \tag{3}$$

and (2) produces $\mu_l \equiv 0$. Equations (1)–(3) are specified in terms of elastic materials; however, the *correspondence principle* permits the material parameters to become complex-valued such that these expressions also apply to viscoelastic materials [53]. Finally, we note that (3) is equivalent to Wood's mixture law, which is often employed in ocean acoustics to determine the sound speed when bubbles are present [54].

To proceed with the first step of the inversion, we assume that a measured compressional sound speed in a fluid-saturated clot, c_m, will be proportional to the speed of sound in the saturating fluid such that $c_m = \delta c_f$. This assumption may be justified by comparing the sound speed of $c_f = 1530$ m/s given in Section 2.6 with the value of 1538 ± 0.2 m/s at 30°C reported by Everbach [55] for clotted human blood plasma. Furthermore, as discussed in Section 2.1, the porosity of blood clots suggests that a fluid-saturated clot may be considered fluid-like, and we have

$$c_m^2 \equiv K_m/\rho_m = \delta^2 K_f/\rho_f = \delta^2 c_f^2, \tag{4}$$

$$\rho_m \equiv (1 - \beta)\rho_e + \beta\rho_f, \tag{5}$$

where ρ_m and K_m represent the effective properties of the fluid-like clot. The subscript "m" denotes "effective quantities" associated with a fluid-saturated clot. Combining Eqs. (3) and (4) and some algebra yields

$$\frac{K_f}{K_e} = \frac{1}{1 - \beta}\left(\frac{\rho_f}{\delta^2 \rho_m} - \beta\right), \tag{6}$$

where constituent one corresponds to the saturating fluid ($c_1 = \beta$, $K_1 = K_f$, and $\mu_1 \equiv 0$) and constituent two corresponds to an isolated fibrin fiber ($c_2 = 1 - \beta$, $K_2 =$

K_e, and $\mu_2 = \mu_e$). To reiterate, Eq. (6) gives the bulk modulus of an isolated fibrin fiber, K_e. The overriding assumptions are that the lower Hashin-Shtrikman bound applies and that the measured compressional sound speed in a fluid-saturated clot is linearly related to the speed of sound in the saturating fluid. The proportionality constant, δ, is considered a free parameter. However, its value is constrained by the ordering of K_f and K_e imposed by the HS bounds.

The next step in the inversion requires placing a constraint on the effective shear rigidity of a saturated clot based on the measured results discussed in Section 2.8. We first set β to the value indicated in Table 1, and using Eq. (6) we adjusted δ to yield values for the ratio K_f/K_e. The values in the first four rows were determined by targeting a value of $K_f/K_e = 0.1$ and in the last four rows by targeting $K_f/K_e = 0.5$. We have no *a priori* means of selecting a value for K_f/K_e; $K_f/K_e = 0.1$ coincides with a K_e value in the neighborhood of steel and 0.5 to a K_e value only twice that of the saturating fluid. From the values for this ratio and $K_f = 2400$ mPa, we determined the values of K_e shown in column 4. The consequences of choosing K_e based on $K_f/K_e = 0.5$ or 0.1 are discussed further below.

Table 1. Parameters values used in and obtained from the inversion to determine K_b and N for a fluid-saturated clot; β is the porosity of the poroelastic medium, δ is a proportionality constant, K_e and μ_e are estimates of the elastic moduli of fibrin, K_m and μ_m are estimates of the elastic moduli of a fluid-saturated clot, and K_b and N are the moduli for a drained clot.

Clot Type	β	δ	K_e (MPa)	μ_e (kPa)	K_m (MPa)	μ_m (Pa)	K_b (Pa)	N (Pa)
Whole	0.90	1.03462	23980	22.27	2637	300.1	350.8	228.6
Plasma	0.97	1.00975	23880	227.3	2467	800.2	947.7	621.9
Fine	0.99	1.00320	23950	353.6	2422	400.0	475.4	312.5
Coarse	0.99	1.00320	23950	884.1	2422	1000.1	1189	781.3
Whole	0.90	1.01262	4802	22.27	2526	300.1	350.8	228.6
Plasma	0.97	1.00359	4799	227.3	2437	800.2	947.7	621.9
Fine	0.99	1.00118	4800	353.6	2412	400.0	475.4	312.5
Coarse	0.99	1.00118	4800	884.1	2412	1000.0	1188	781.3

The values in the last five columns in Table 1 were determined by applying Berryman's self-consistent effective medium theory to a fluid-saturated clot. A detailed discussion of this procedure can be found elsewhere [48, 49]; we merely quote results for a two-constituent composite elastic medium with needle-like inclusions:

$$c_1(K_1 - K_m)P_{1m} + c_2(K_2 - K_m)P_{2m} = 0, \tag{7}$$

$$c_1(\mu_1 - \mu_m)Q_{1m} + c_2(\mu_2 - \mu_m)Q_{2m} = 0, \tag{8}$$

$$P_{1m} = \frac{K_m + \mu_m + \mu_1/3}{K_1 + \mu_m + \mu_1/3}, \tag{9}$$

$$Q_{1m} = \frac{1}{5}\left(\frac{4\mu_m}{\mu_m + \mu_1} + 2\frac{\mu_m + \gamma_m}{\mu_1 + \gamma_m} + \frac{K_1 + 4\mu_m/3}{K_1 + \mu_m + \mu_1/3}\right), \tag{10}$$

$$\gamma_m = \mu_m \frac{3K_m + \mu_m}{3K_m + 7\mu_m}. \tag{11}$$

We note that the self-consistent moduli satisfy the rigorous lower and upper Hashin-Shtrikman bounds. Again, the subscript "m" designates that the quantity is a property of the "effective medium." Equations (7) through (11) are solved using a iterative technique, and P_{2m} and Q_{2m} are determined from substitution of appropriate subscripts in Eqs. (9) and (10).

In Eqs. (7) through (11), we set $c_1 = \beta$, $K_1 = K_f$, $\mu_1 = 0$, $c_2 = 1 - \beta$, and $K_2 = K_e$. This leaves the value of $\mu_2 = \mu_e$ (the shear rigidity of an isolated fibrin fiber) as a free parameter. We adjusted the value of μ_e to arrive at values for K_m and μ_m (columns 6 and 7 of Table 1) such that the value of μ_m was constrained by the real part of the experimentally determined values discussed in Section 2.8 for the various types of fluid-saturated blood clots. Using Eqs. (4) and (5) with the tabulated values of K_m, we predicted a speed of sound for various fluid-saturated clots that satisfied constraints on δ.

In the final step of the inversion, we applied the self-consistent effective medium theory again, but in this case the saturating fluid had been removed. Hence, $c_1 = \beta$, $K_1 = \mu_1 = 0$, $c_2 = 1 - \beta$, and we used the estimates of K_e and μ_e for an isolated fibrin fiber in a fluid-saturated clot to obtain new estimates of K_m and μ_m which, in turn, provided estimates $K_b \equiv K_m$ and $N \equiv \mu_m$ for the drained skeletal frame (last two columns of Table 1). Clearly, the estimated values of N are consistent with the values reported in Section 2.8. This is expected because assuming that the saturating fluid is inviscid means that the network of fibrin fibers provides the only contribution to the shear rigidity of a clot.

The inversion procedure assumes that the material parameters are real valued to simplify the analysis. This yields real-valued estimates for K_e, K_b, and N. The measured values reported in Section 2.8 for the shear rigidity of a saturated clot contain a small imaginary component due to intrinsic absorption. Absorption arises from viscous flow within the pore space and intrinsic absorption with the fibrin. The absorption from viscous flow is included explicitly within Biot's theory through a dissipation function that depends on the viscosity and hydrostatic permeability of the fluid. The intrinsic absorption in the fibrin is included by augmenting the estimate of N by an imaginary component based on the discussion given in Section 2.8.

3. RESULTS

Detailed discussion of the material parameters and mathematical formalism for Biot's theory has been given by Kargl and Lim [23] and Kargl et al. [22] and will not be repeated here. They reduce the governing equations for wave propagation to dispersion relations for compressional and shear waves. As mentioned previously, one consequence of Biot's theory is the possibility of two distinct compressional modes of propagation (i.e., a fast wave and a slow wave). Using the values of K_e, K_b, the real part of N tabulated in Table 1, and the average parameters listed in Table 2, we computed the phase velocities and the absorption coefficients for the various clot types. In these computations, the ratio of the imaginary part of N to its real part was consistent with the measured values reviewed in Section 2.8.

Table 2. Parameters used to compute the phase velocities and absorption coefficients for the various clot types. The values in rows 4–10 were obtained from the inversion procedure described in Section 2.9

	Whole blood	Plasma	Coarse fibrin	Fine fibrin	Unit
β	0.90	0.97	0.99	0.99	
K_d	1.0	0.1	0.5	0.006	$\times 10^{-12}$ m^2
α	1.1	1.03	1.01	1.01	
ρ_f	1027	1027	1027	1027	kg/m^3
K_f	2400	2400	2400	2400	MPa
η	1.04	1.04	1.04	1.04	mPl
ρ_e	1300	1300	1300	1300	kg/m^3
K_e	23980	23880	23950	23950	MPa
K_b	350.8	947.7	1189	475.4	Pa
N	$228.6 - i7.6$	$621.9 - i155.5$	$781.3 - i78.1$	$312.5 - i62.5$	Pa

Figure 1 shows the phase velocities of the three acoustic waves predicted to occur within a whole-blood clot by Biot's theory as a function of frequency. Those phase velocities have been normalized by the sound speed in the saturating liquid, c_f = 1530 m/s, and vary weakly with frequency. The phase velocity of the fast wave depends almost entirely on the acoustic properties of the saturating fluid (i.e., the fluid's bulk modulus and density), because its value is close to that calculated for acoustic wave propagation in 100% fluid. The phase velocity of the fast wave is 1582.2 ± 0.25 m/s over the frequency range depicted in Figure 1. The phase velocities of the slow and shear waves are significantly smaller than that of the fast wave, suggesting that sound incident on a blood clot of finite extent would couple weakly into the slow and shear waves and almost exclusively into the fast wave. This computation was performed using the set of material parameters for whole blood listed in the first

column of Table 2. If we use the K_e, K_b, and N values listed in the fifth row of Table 1, for which K_e is significantly different, the results are essentially the same. Thus, within the Biot paradigm, we conclude that the acoustic properties of fluid-saturated blood clots appear relatively insensitive to the bulk modulus of an isolated fibrin fiber.

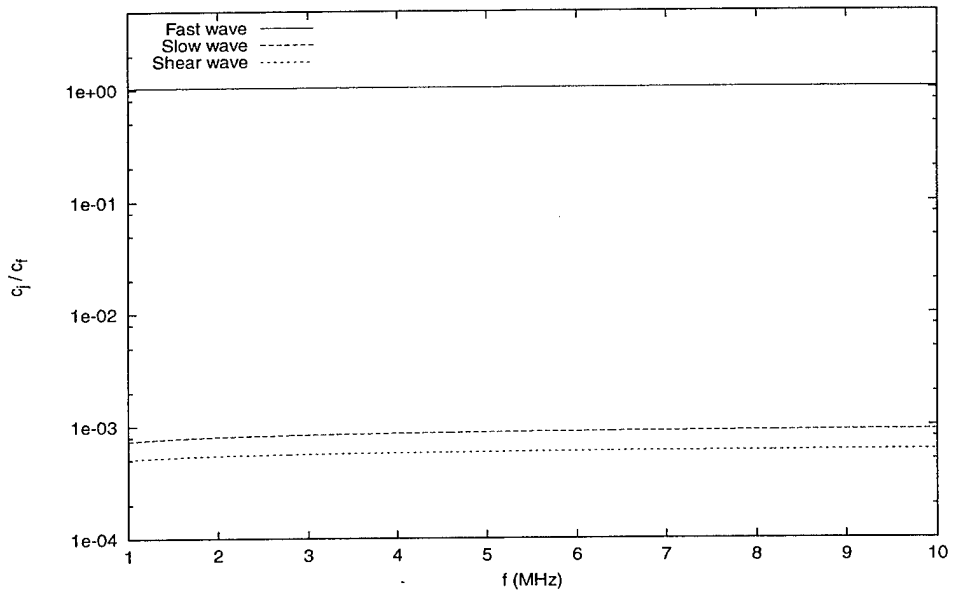

Figure 1. Normalized phase velocities, c_j/c_f, for wave propagation in a whole-blood clot. Note that the phase velocities are weakly dispersive. The fast wave propagates at nearly the speed of sound in pure serum, and the slow and shear waves propagate at much slower speeds. The phase velocities have been normalized by the speed of sound in serum, $c_f = 1530$ m/s.

Figure 2 shows the absorption coefficient for the three waves as a function of frequency. The absorption coefficient is simply the imaginary part of the wavenumber. The primary energy dissipation mechanisms are thermoviscous attenuation due to relative motion of the underlying constituents and intrinsic losses characterized by complex moduli. The extremely large values for the slow and shear waves demonstrate that these waves are essentially diffusive in character, and hence do not propagate to any extent before completely attenuating.

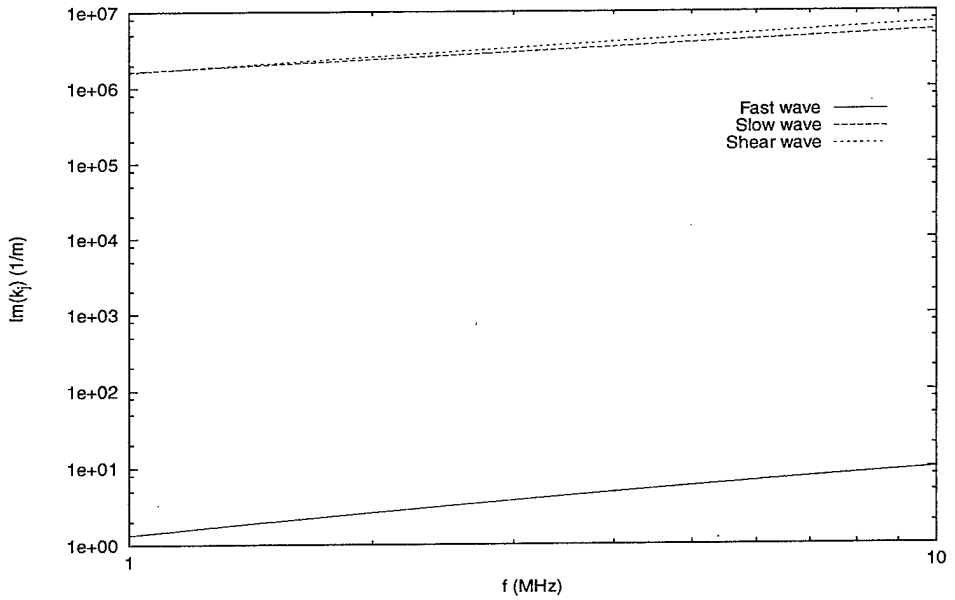

Figure 2. Absorption coefficients for a whole-blood clot. The absorption coefficient is simply the imaginary component of the wave number, k_j. The large values for the slow and shear waves suggest that these waves are diffusive in character.

The results for the other clot types are similar to those shown in Figures 1 and 2. Because the speed of the fast wave depends almost entirely on the properties of the fluid, as discussed previously, by showing the value for whole blood we effectively do so for all of the blood-clot types. The slow and shear-wave sound speeds computed for the other clot types exhibit more dispersion than observed in the computations for the whole-blood clot but are generally of the same magnitude. Moreover, the diffusive character found in the whole-blood clot for the slow and shear waves is also found in these clots. Thus it is clear that little energy will be coupled into the slow and shear waves, and any sound speed measured in a clot will be that of the fast wave.

4. CONCLUSIONS

We have applied Biot's theory to the problem of acoustic wave propagation in fluid-saturated clots. This theory requires at least ten material parameters, and we have surveyed the literature for representative values. Section 2 contains a summary of these parameters, which were culled from a variety of sources, none of which had the Biot paradigm in mind. Indeed, in Section 2.9 we have to resort to an inversion procedure to estimate the bulk modulus of an isolated fibrin fiber and the bulk modulus of the drained skeletal frame. Moreover, some of the reported parameter values have shortcomings, as discussed in Section 2. Particularly needed are refinements of the measures of the bulk moduli and density of fibrin. Therefore, our results should be considered as a first attempt to represent via Biot's theory the acoustic propagation within blood clots.

Figures 1 and 2 suggest that neither a slow wave nor a shear wave may be directly observable in a blood clot. One might then conclude that Biot's theory is an inappropriate model for the wave propagation. However, even though the slow and shear waves may be unobservable, a salient feature of the readily observable fast wave is the relative motion of the saturating fluid with respect to the network of fibrin fibers. A preliminary computation [56] of the relative displacement of the fluid constituent per acoustic cycle yields a peak displacement on the order of 1–10 nm, which rivals the distances between binding sites within fibrin meshes [57]. Hence the application of ultrasound during enzyme-mediated thrombolysis may accelerate thrombolysis through advective and diffusive transport of a clot-lysing agent, rather than by diffusion alone.

In this report, we have focused on the material parameters for fluid-saturated blood clots and their phase velocities and absorption coefficients in a bulk medium. In practice, bloods clots are of finite extent, and thus boundaries become important. In addition to the importance of the relative displacement of fluid, we are currently studying the stresses associated with the displacements and reflection and transmission coefficients at planar boundaries. The details of that study, which makes use of the information gathered here, will be reported elsewhere. However, at standard medical ultrasound frequencies, we find that sound incident on a blood clot will couple primarily into the fast wave, with much weaker coupling into the slow wave and insignificant coupling into the shear wave [56]. Again, we have not shown that Biot's theory is irrelevant for the interaction of blood clots and sound because the fast wave has properties significantly different from those of compressional waves within pure liquids or pure elastic solids. In particular, there is relative motion of the saturating fluid and fibrin frame. Also, the slow wave can be excited at interfaces, which suggests that the slow wave may enhance transport of a clot-lysing agent across interfaces. These properties may be important for understanding possible biological effects

of sound propagation within blood clots, including answering how ultrasound-assisted thrombolysis occurs without the action of bubbles or heat, as briefly described in the introduction.

Understanding the bio-effects implicit in an application of Biot's theory to sound propagation in blood clots and to ultrasound-assisted thrombolysis will take careful and perhaps subtle analysis and experiments. In particular, experiments addressing how Biot's theory can help explain ultrasound-assisted thrombolysis should be made from whole blood or from fibrin gels that incorporate erythrocytes, and careful measurements of all relevant material properties are required.

REFERENCES

[1] C. W. Francis, P. T. Onundarson, E. L. Carstensen, A. Blinc, R. S. Meltzer, K. Schwarz, and V. J. Marder, "Enhancement of fibrinolysis in vitro by ultrasound," *J. Clin. Invest.*, **90**, 2063–2068 (1992).

[2] C. G. Lauer, R. Burge, D. B. Tang, B. G. Bass, E. R. Gomez, and B. M. Alving, "Effect of ultrasound on tissue-type plasminogen activator-induced thrombolysis," *Circulation*, **86**, 1257–1264 (1992).

[3] C. M. Sehgal, R. F. Leveen, and R. D. Shlansky-Goldberg, "Ultrasound-assisted thrombolysis," *Invest. Radiol.*, **28**, 939–943 (1993).

[4] H. Luo, W. Steffen, B. Cercek, S. Arunasalam, G. Maurer, and R. J. Siegel, "Enhancement of thrombolysis by external ultrasound," *Am. Heart J.*, **125**, 1564–1569 (1993).

[5] A. Blinc, C. W. Francis, J. L. Trudnowski, and E. L. Carstensen, "Characterization of ultrasound-potentiated fibrinolysis in vitro," *Blood*, **81**, 2636–2643 (1993).

[6] F. Siddiqi, A. Blinc, J. Braaten, and C. W. Francis, "Ultrasound increases flow through fibrin gels," *Thrombosis and Haemostasis*, **73**, 495–498 (1995).

[7] A. Blinc and C. W. Francis, "Transport processes in fibrinolysis and fibrinolytic therapy," *Thrombosis and Haemostasis*, **76**, 481–491 (1996).

[8] S. Kudo, "Thrombolysis with ultrasound effect," *Tokyo Jikeikai Med. J.*, **104**, 1005–1012 (1989).

[9] R. Kornowski, R. S. Meltzer, A. Chernine, Z. Vered, and A. Battler, "Does external ultrasound accelerate thrombolysis? Results from a rabbit model," *Circulation*, **89**, 339–344 (1994).

[10] A. Kashyap, A. Blinc, V. J. Marder, D. P. Penney, and C. W. Francis, "Acceleration of fibrinolysis by ultrasound in a rabbit ear model of small vessel injury," *Thromb. Res.*, **76**, 475–485 (1994).

[11] H. Luo, T. Nishioka, M. C. Fishbein, B. Cercek, J. S. Forrester, C. J. Kim, H. Berglund, and R. J. Siegel, "Transcutaneous ultrasound augments lysis of arterial thrombi in vivo," *Circulation*, **94**, 775–778 (1996).

[12] S. L. Poliachik, W. L. Chandler, P. D. Mourad, M. R. Bailey, S. Bloch, R. O. Cleveland, P. Kaczkowski, G. Keilman, T. Porter, and L. A. Crum, "Effect of

high intensity focused ultrasound on whole blood with and without microbubble contrast agent," *Ultra. Med. Bio.*, **25**, 991–998 (1999).

[13] E. C. Everbach, J. White, and C. W. Francis, "Overpressure reduces acceleration of thrombolysis due to ultrasound," *J. Acoust. Soc. Am.*, **102**, 3154(A) (1997).

[14] C. W. Francis, V. Suchkova, and E. C. Everbach, "Enhancement of fibrinolysis by low-intensity c.w. ultrasound," *J. Acoust. Soc. Am.*, **105**, 1369(A) (1999).

[15] G. A. Shah, I. A. Ferguson, T. Z. Dhall, and D. P. Dhall, "Polydispersion in the diameter of fibers in fibrin networks: Consequences on the measurement of mass-strength ratio by permeability and turbidity," *Biopolymers*, **21**, 1037–1047 (1982).

[16] M. A. Biot, "Theory of propagation of elastic waves in a fluid saturated porous solid. I. Low frequency range," *J. Acoust. Soc. Am.*, **26**, 168–178 (1956).

[17] M. A. Biot, "Theory of propagation of elastic waves in a fluid saturated porous solid. II. High frequency range," *J. Acoust. Soc. Am.*, **26**, 179–191 (1956).

[18] T. J. Plona, "Observations of a second bulk compressional wave in a porous medium at ultrasonic frequencies," *Appl. Phys. Lett.*, **36**, 259–261 (1980).

[19] R. D. Stoll and T.-K. Kan, "Reflection of acoustic waves at a water-sediment interface," *J. Acoust. Soc. Am.*, **70**, 149–156 (1981).

[20] D. L. Johnson, "Elastodynamics of gels," *J. Chem. Phys.*, **77**, 1531–1539 (1982).

[21] D. L. Johnson, "Recent developments in the acoustic properties of porous media," in *Frontiers of Physical Acoustics, International School of Physics Enrico Fermi, Course XCIII*, edited by D. Sette (North-Holland, Amsterdam, 1986), pp. 255–290.

[22] S. G. Kargl, K. L. Williams, and R. Lim, "Double monopole resonance of a gas-filled, spherical cavity in a sediment," *J. Acoust. Soc. Am.*, **103**, 265–274 (1998).

[23] S. G. Kargl and R. Lim, "A transition-matrix formulation of the scattering in homogeneous, saturated, porous media," *J. Acoust. Soc. Am.*, **94**, 1527–1550 (1993).

[24] R. W. Rosser, W. W. Roberts, and J. D. Ferry, "Rheology of fibrin clots. IV. Darcy constants and fiber thickness," *Biophysical Chemistry*, **7**, 153–157 (1977).

[25] S. Anand, J.-H. Wu, and S. L. Diamond, "Enzyme-mediated proteolysis of fibrous biopolymers: Dissolution of front movement and fibrin or collagen under conditions of diffusive or convective transport," *Biotech. Bioeng.*, **48**, 89–107 (1995).

[26] M. Okada and B. Blomback, "Factors influencing fibrin gel structure studied by flow measurement," *Annals New York Acad. Sci.*, **408**, 233–253 (1983).

[27] M. E. Carr and C. L. Hardin, "Fibrin has larger pores when formed in the presence of erythrocytes," *Am. J. Physio.*, **253**, H1069–H1073 (1987).

[28] M. E. Carr, L. L. Shen, and J. Hermans, "Mass-length ratio of fibrin fibers from gel permeation and light scattering," *Biopolymers*, **16**, 1–15 (1977).

[29] F. A. Duck, *Physical Properties of Tissue, A Comprehensive Reference Book* (Academic, London, 1990).

[30] W. C. Watson, "Lipaemia, heparin, and blood viscosity," *The Lancet*, **6991**, 366–368 (1957).

[31] M. A. Shearn, W. V. Epstein, and E. P. Engleman, "Serum viscosity in rheumatic diseases and macroglobulinemia," *Archives Int. Med.*, **112**, 684–687 (1963).

[32] M. A. Shearn, W. V. Epstein, and E. P. Engleman, "Relationship of serum proteins and rheumatoid factor to serum viscosity in rheumatic diseases," *J. Lab. Clin. Med.*, **61**, 667–686 (1963).

[33] R. S. Rosenson, A. McCormick, and E. F. Uretz, "Distribution of blood viscosity values and biochemical correlates in healthy adults," *Clin. Chem.*, **42**, 1189–1195 (1996).

[34] E. W. Merrill and R. E. Wells, "Flow properties of biological fluids," *Appl. Mech. Rev.*, **14**, 663–673 (1961).

[35] E. L. Carstensen and H. P. Schwan, "Acoustic properties of hemoglobin solutions," *J. Acoust. Soc. Am.*, **31**, 305–311 (1959).

[36] A. F. Collings and N. Bajenov, "Temperature dependence of the velocity of sound in human blood and blood components," *Australasian Phys. Eng. Sci. Medicine*, **10**, 123–127 (1987).

[37] A. E. Aubert, H. Kesteloot, and H. de Geest, "Measurement of high frequency sound velocity in blood," *Biosigma 78*, **1**, 421–425 (1978).

[38] J. D. Ferry and P. R. Morrison, "Preparation and properties of serum and plasma proteins. IX. Human fibrin in the form of an elastic film," *J. Amer. Chem.*, **69**, 400–408 (1947).

[39] W. A. Voter, C. Lucaveche, and H. P. Erickson, "Concentration of protein in fibrin fibers and fibrinogen polymers determined by refractive index matching," *Biopolymers*, **25**, 2375–2384 (1986).

[40] M. Kaibara, E. Fukada, and K. Sakaoku, "Rheological study on network structure of fibrin clots under various conditions," *Biorheology*, **18**, 23–35 (1981).

[41] M. Kaibara and E. Fukada, "Dynamic viscoelastic study for the structure of fibrin networks in the clots of blood and plasma," *Biorheology*, **6**, 329–339 (1970).

[42] K. A. Overholser, J. P. Itin, D. R. Brown, and T. R. Harris, "The effect of herparin on the viscoelasticity of whole blood clots," *Biorheology*, **12**, 309–316 (1975).

[43] M. Kaibara and E. Fukada, "The influence of the concentration of thrombin on the dynamic viscoelasticity of clotting blood and fibrinogen-thrombin systems," *Biorheology*, **8**, 139–147 (1971).

[44] G. W. Kamykowski, D. F. Mosher, L. Lorand, and J. D. Ferry, "Modification of shear modulus and creep compliance of fibrin clots by fibronectin," *Biophys. Chem.*, **13**, 25–28 (1981).

[45] M. Kaibara and E. Fukada, "Non-Newtonian viscosity and dynamic viscoelasticity of blood during clotting," *Biorheology*, **6**, 73–84 (1969).

[46] G. W. Nelb, G. W. Kamykowski, and J. D. Ferry, "Rheology of fibrin clots. V. Sheer modulus, creep, and creep recovery of fine unligated clots," *Biophy. Chem.*, **13**, 15–23 (1981).

[47] M. D. Bale, M. F. Muller, and J. D. Ferry, "Rheological studies of creep and creep recovery of unligated fibrin clots: comparison of clots prepared with thrombin and ancrod," *Biopolymers*, **24**, 461–482 (1985).

[48] J. G. Berryman, "Long-wavelength propagation in composite elastic media. I: Spherical inclusions," *J. Acoust. Soc. Am.*, **68**, 1809–1819 (1980).

[49] J. G. Berryman, "Long-wavelength propagation in composite elastic media. II: Ellipsoid inclusions," *J. Acoust. Soc. Am.*, **68**, 1820–1831 (1980).

[50] Z. Hashin and S. Shtrikman, "Note on a variational approach to the theory of composite elastic materials," *J. Franklin Inst.*, **271**, 336–341 (1961).

[51] Z. Hashin and S. Shtrikman, "On some variational principles in anisotropic and nonhomogeneous elasticity," *J. Mech. Phys. Solids*, **10**, 335–342 (1962).

[52] Z. Hashin and S. Shtrikman, "A variational approach to the theory of the elastic behaviour of multiphase materials," *J. Mech. Phys. Solids*, **11**, 127–140 (1963).

[53] M. J. Leitman and G. M. C. Fisher, "The linear theory of viscoelasticity," in *Handbuch der Physik*, edited by C. Truesdell (Springer-Verlag, New York, 1973), vol. VIa/3, pp. 1–123.

[54] R. J. Urick, *Principles of Underwater Sound for Engineers* (McGraw-Hill, New York, 1975).

[55] E. C. Everbach, Tissue composition determination via measurement of the acoustic nonlinearity parameter, Ph.D. thesis, Yale University, 1989.

[56] P. D. Mourad and S. G. Kargl, "Are blood clots a biot medium?" in *16th Inter. Cong. on Acoust. and 135th Meeting of the Acoust. Soc. of Amer.* (Acoust. Soc. Amer., Seattle, WA, 1998), vol. IV, pp. 2501–2502.

[57] R. R. Hentgen, C. W. Francis, and V. J. Marden, "Fibrogen structure and physiology," in *Hemostatis and Thrombolysis: Basic Principles and Clinical Practices*, edited by R. W. Coleman, J. Hirsh, V. J. Marden, and E. W. Salzman (Lippincott, Philadelphia, 1994), p. 1713.

REPORT DOCUMENTATION PAGE

Form Approved
OPM No. 0704-0188

1. AGENCY USE ONLY *(Leave blank)*	2. REPORT DATE	3. REPORT TYPE AND DATES COVERED
	September 2000	Technical

4. TITLE AND SUBTITLE

Acoustic Properties of Fluid-Saturated Blood Clots

5. FUNDING NUMBERS

ONR Contract N00014-96-1-0630

6. AUTHOR(S)

Pierre D. Mourad and Steven G. Kargl

7. PERFORMING ORGANIZATION NAME(S) AND ADDRESS(ES)

Applied Physics Laboratory
University of Washington
1013 NE 40th Street
Seattle, WA 98105-6698

8. PERFORMING ORGANIZATION REPORT NUMBER

APL-UW TR 2003

9. SPONSORING / MONITORING AGENCY NAME(S) AND ADDRESS(ES)

Office of Naval Research
Ballston Tower 1
800 North Quincy Street
Arlington VA 22217-5660

10. SPONSORING / MONITORING AGENCY REPORT NUMBER

11. SUPPLEMENTARY NOTES

Approved for public release; distribution is unlimited.

12a. DISTRIBUTION / AVAILABILITY STATEMENT

Approved for public release; distribution is unlimited.

12b. DISTRIBUTION CODE

13. ABSTRACT *(Maximum 200 words)*

Ultrasound has been applied to blood clots to enhance enzyme-mediated thrombolysis through unknown mechanisms. A basic physical description of a blood clot is a two-phase medium composed of a saturating fluid and an interconnected network of elastic material. Acoustic wave propagation in a fluid-saturated, poroelastic medium can be represented by Biot's theory. The question therefore arises, Might blood clots support the propagation of sound in a way consistent with Biot's theory? We address this question by first surveying the literature for measurements of the physical properties of blood clots that are needed to apply Biot's theory. We discuss the strengths and weaknesses of these measurements, and determine a useful set of values for modeling. Using these parameter values, we then calculate the phase velocities and absorption coefficients of the three waves predicted by Biot's theory for various types of blood clots in an unbounded medium.

14. SUBJECT TERMS

Ultrasound, blood clots, thrombolysis, Bio theory, properties of thrombi

15. NUMBER OF PAGES

27

16. PRICE CODE

17. SECURITY CLASSIFICATION OF REPORT	18. SECURITY CLASSIFICATION OF THIS PAGE	19. SECURITY CLASSIFICATION OF ABSTRACT	20. LIMITATION OF ABSTRACT
Unclassified	Unclassified	Unclassified	SAR